

# Observations on Experimental Fluid Structure Interactions of Plate-Type Fuel

W. Marcum<sup>1\*</sup>, A.M. Phillips<sup>2</sup>, W.F. Jones<sup>2</sup>, A.W. Weiss<sup>1</sup>, T.K. Howard<sup>1</sup>

1) School of Nuclear Science and Engineering, Oregon State University, 116 Radiation Center, Corvallis OR 97331, USA

2) Fuels Development Program, Idaho National Laboratory, Idaho Falls ID 83415, USA

Corresponding author: [wade.marcum@oregonstate.edu](mailto:wade.marcum@oregonstate.edu)

**Abstract.** The Materials Management and Minimization Program is pursuing the goal of converting all United States nuclear civilian research and test reactors from highly enriched uranium to low enriched uranium (LEU) fuel. At present 49 reactors have successfully been converted, leaving five reactors yet to have their fuel changed. These five reactors have much higher neutron fluxes than their counterparts and as such have been termed ‘high performance research reactors’ (HPRRs). Presently qualified fuel options in LEU composition would significantly reduce these reactors’ performance characteristics. As such, the Fuels Development Program led by the Idaho National Laboratory (INL) is presently working to qualify a new ultra-high-density LEU fuel composition consisting of a monolithic uranium molybdenum alloy. A necessary activity to support the qualification of this fuel is to characterize the prototypic fuel’s mechanical response under hydraulically loaded conditions. Oregon State University is working in collaboration with the INL to perform a comprehensive set of flow tests in a large-scale flow loop with this prototypic fuel as well as alternate materials. The element to be tested has been termed the Generic Test Plate Assembly (GTPA) as it is not representative of physical attributes of any of the HPRRs, but rather is designed to prescribe well-known boundary conditions on a series of flat test plates. This comprehensive testing campaign includes a statistically significant number of tests for each independent variable considered. In this case, three independent variables are investigated, the response of plates that (1) comprise aluminum 6061-T0, (2) are aluminum clad and have a surrogate material (stainless steel) dispersed within the fuel-meat region, and (3) are aluminum clad and have a monolithic DU10Mo fuel meat region. The objectives of this parametric testing effort are to (1) demonstrate the relative difference in mechanical response of each material type, (2) develop an experimental data-set that is of the quality, rigor, and resolution to support the validation of modelling tools, and (3) develop a better understanding of the mechanical instabilities of plate-type fuel under extreme hydraulic loading.

In order to satisfy these objectives the testing program is utilizing state-of-the-art instrumentation to characterize material properties, hydraulic boundary conditions, and mechanical response before, during, and after flow testing. While the testing campaign is early in its execution, a number of substantiated observations have been made that already shed light on objectives 2 and 3 detailed above. This paper presents the methods, outcomes, and observations made from these early NQA-1 compliant flow tests, demonstrating a successful observation of plastic deformation of this plate-type fuel and a basis for its occurrence when compared against previous computational studies’ results.

## 1 Introduction

The Materials Management and Minimization Program is pursuing the goal of converting all United States nuclear civilian research and test reactors from highly enriched uranium to low enriched uranium (LEU) fuel. At present 49 reactors have successfully been converted, leaving five reactors yet to have their fuel changed. These five reactors have much higher neutron fluxes than their counterparts and as such have been termed ‘high performance research reactors’ (HPRRs). Presently qualified fuel options in LEU composition would significantly reduce these reactors’ performance characteristics. As such, the Fuels Qualification Program led by the Idaho National Laboratory (INL) is presently working to qualify a new ultra-high-density LEU fuel composition consisting of a monolithic uranium molybdenum alloy. A necessary activity to support the qualification of this fuel is to characterize the prototypic fuel’s mechanical response under hydraulically loaded conditions.

Oregon State University is working in collaboration with the INL to perform a comprehensive set of flow tests in a large-scale flow loop with this prototypic fuel as well as alternate materials. The element to be tested has been termed the Generic Test Plate Assembly (GTPA) as it is not representative of physical attributes of any of the HPRRs, but rather is designed to prescribe well-known boundary conditions on a series of flat test plates. This comprehensive testing campaign includes a statistically significant number of tests for each independent variable considered. In this case, three independent variables are investigated, the response of plates that (1) comprise aluminum 6061-T0, (2) are aluminum clad and have a surrogate material (stainless steel) dispersed within the fuel-meat region, and (3) are aluminum clad and have a monolithic DU10Mo fuel meat region. The objectives of this parametric testing effort are to (1) demonstrate the relative difference in mechanical response of each material type, (2) develop an experimental data-set that is of the quality, rigor, and resolution to support the validation of modelling tools, and (3) develop a better understanding of the mechanical instabilities of plate-type fuel under extreme hydraulic loading.

In order to satisfy these objectives the testing program is utilizing state-of-the-art instrumentation to characterize material properties, hydraulic boundary conditions, and mechanical response before, during, and after flow testing. While the testing campaign is early in its execution, a number of substantiated observations have been made that already shed light on objectives 2 and 3 detailed above. This paper presents the methods, outcomes, and observations made from these early NQA-1 compliant flow tests, demonstrating a successful observation of plastic deformation of this plate-type fuel and a basis for its occurrence when compared against previous computational studies' results.

## 2 Experimental Description

The OSU HMFTF has been designed to operate under a large range of thermal hydraulic conditions which are elevated well above that of an ambient state.

### 2.1 Loop Description

The experimental data collected as a part of this test program is done so through use of the HMFTF located at OSU. The HMFTF is a thermal hydraulic test loop. The current design of the HMFTF permits for hydraulic testing of a wide range of components. This study focuses on testing of the generic test plate assembly. The OSU HMFTF caters to a broad range of operating conditions as seen in Table I [1]. Because the HMFTF's purpose is providing hydro-mechanical information, its design is currently limited to sub-cooled isothermal testing capabilities.

*Table I – HMFTF fluid operating range*

Parameter	Value
Flow Rate Range [liters/sec]	0 – 100.94
Pressure Range [MPa]	0.101 – 4.137
Fluid Temperature Range [°C]	20 – 238
Conductivity Range [micromhos]	1 – 3
pH Range	4 – 8

The HMFTF test section is approximately 2.56 m (8.42 ft) in total length. Discrete locations along the length of the test section pipe are made available for the insertion of electrical wire

leads for strain gages, pitot tubes for pressure transmitters, pressure indicating flow transmitters, and other hydraulic instrumentation as deemed necessary for a particular test.

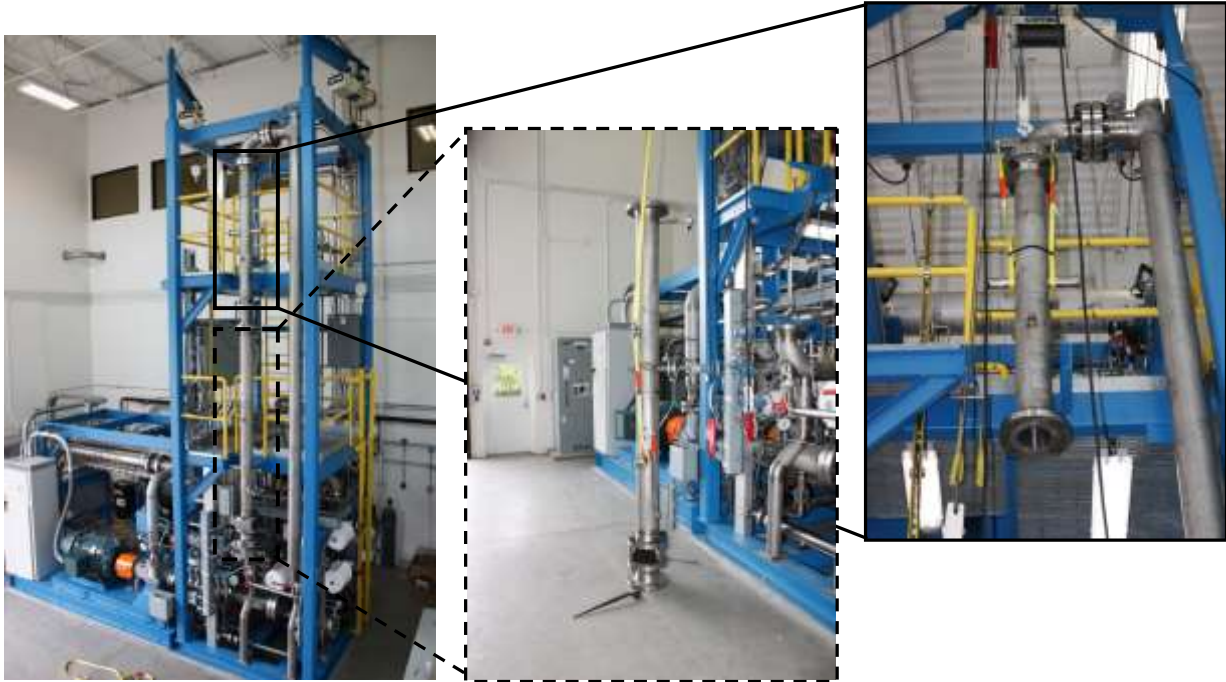


FIG 1 – Picture of HMFTF (left), test section (center) and flow straightener (right)

The test section is designed to provide a flexible interface for any desired test element which meets overall size criteria. This is achieved by designing individual test section element-specific inserts which mate directly with the element. The purpose of these inserts is to simulate in-core flow conditions. These inserts are fed into the test section pipe and coupled to a universal interface to secure the insert and the element within the test section. A vaned flow straightener resides upstream of the test section providing for repeatable and well controlled inlet boundary conditions on the test section. The location of the vaned flow straightener and test section are shown in figure 1 within the overall primary loop piping system of the HMFTF. Note that the vaned flow straightener is located above the test section in the figure 1, requiring that the flow direction be downward in the vertical direction through the test section. The benchmark flow test described herein takes place in the downward flow direction, however, orientation is not anticipated to impact experimental results, as the test under discussion will take place in an isothermal environment, negating the influence of buoyancy forces within the test section region.

## 2.2 Test Element Design

The test element, or generic test plate assembly considered herein comprises six flat plates aligned adjacent to one another. This test plate does not physically represent the analogue to any reactor, but rather provides generic and highly controlled boundary conditions for which one may acquire the most accurate and significant outcomes from the experiments for the purpose of comparing various fuelled materials. Each plate is 609.6 mm (24 inches) in length, 101.6 mm (4 inches) in width, and has a total thickness of 1.27 mm (0.05 inches). Five of the six plates within the GTPA are referred to as hydraulic plates. These hydraulic plates are made of hastalloy and are assembled in an array, as shown in figure 2 to provide well-defined hydraulic boundary conditions on the test plate. The hastalloy plates are assembled and

bounded in the fixed edges. The test plate is made of aluminum and bound by piano wire, running the length of each plate edge. These wires, under a light compressive load, serve to provide representative pinned edge boundary conditions. Six of the seven sub-channels in the GTPA are spaced evenly at 1.905 mm (0.075 inches), while the center sub-channel (figure 2) is slightly larger in width than all others at 4.775 mm (0.188 inches). This change in flow geometry biases flow through the center channel, increasing the superficial velocity in that region relative to the others, therefore reducing the local pressure. By creating a pressure differential between the center flow channel and its adjacent flow channels, membrane stresses are created on the fuel plates separating these channels.

Six strain gages are bonded to the test plate in unique axial locations (figure 8) providing discrete, measurement of strain (correlated to deflection through calibration) along the length of the plate. Additionally, a fiber-optic distributed strain sensor is bonded to the back-side of the plate in a serpentine pattern. The fiber-optic distributed strain sensor (DSS) serves to provide distributed strain sensing throughout the breadth of the plate. While the strain gages are limited to single-point measurement, their ability to adequately capture strain at under high-response rates (and therefore resolve spectral characteristics of the plate) is significant with acquisition rates up to 25 kHz, whereas the DSS' limit on acquisition rate is left to 200 Hz. Each of these respective instrument sets compliments one another providing a spatially and temporally resolved response of the plate under steady and transient boundary conditions, as will be detailed hereinafter.

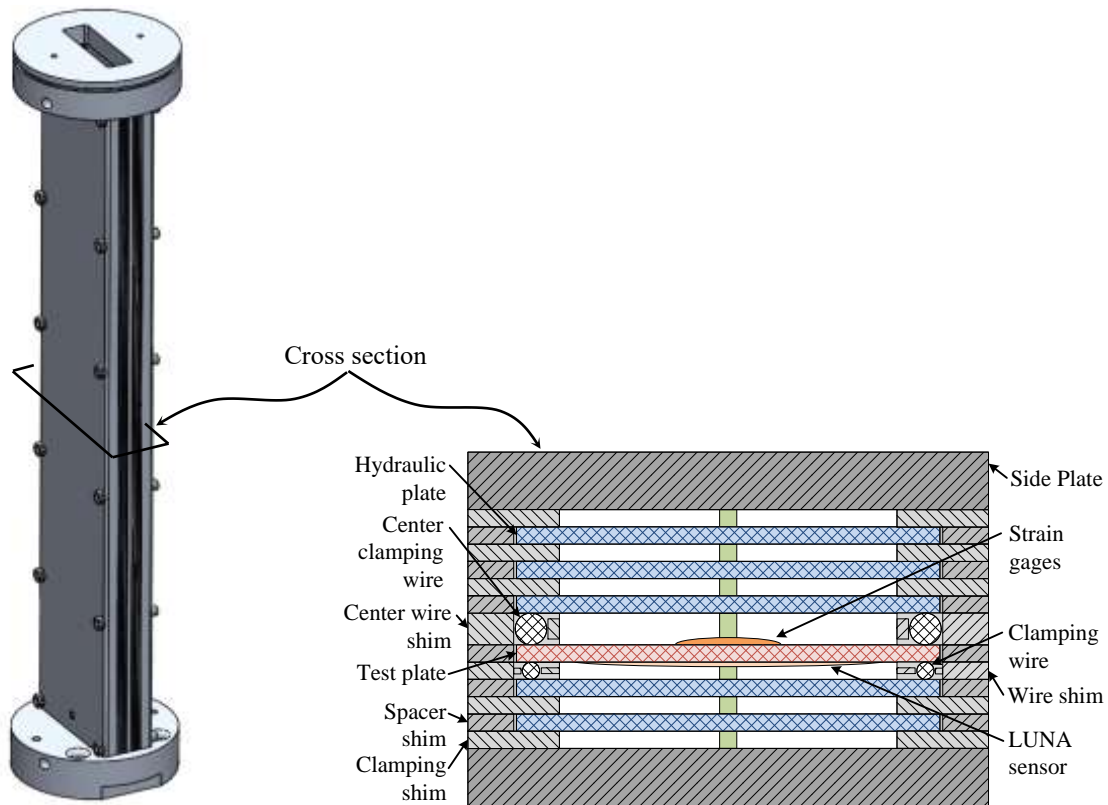


FIG 2 – Geometric layout of the GTPA

The hydraulic instrumentation and measurement techniques used in the HMFTF are similar to those historically employed as a part of plate-type reactor hydraulic characterization [2] and fuel qualification. The GTPA is located near the outlet of the test section. A pitot tube

assembly is hermetically sealed to the test section piping at the outlet of the test section. The test section insert adjacent to the pitot tube assembly has a single slot cut out to allow the pitot tube plate to pass into the flow channel. The insert is aligned in the test section such that a given element's flow channels is approximately 12.7 mm (0.5 in) vertically past the pitot tubes' measurement end. This allows each pitot tube to penetrate inside the element's flow channels 12.7 mm (0.5 in) to acquire the true, local, dynamic pressure associated with that flow channel for a given fluid flow rate and temperature. Total- and static-pressure probes (pitot tubes) are positioned in each flow channel. The open end of the total pressure probe is aligned with the flow direction and is located in the span-wise center of each subchannel, inserted approximately 6.35 mm (0.25) inches inside the channel. By locating each total probe in the span-wise center it can be assumed that its location acquires pressure which reflects that of the maximum coolant velocity passing through the channel. The total pressure probes are located inside (rather than at the outlet of) each flow channel in order to collect representative data of each prescribed channel and filter out large fluctuations in pressure which may occur at the channel outlet where mixing is dominated.

### 3 Results & Discussion

The test detailed herein was performed at a nominal system pressure of 120 psig and fluid temperature of 250 F. Note that British units are presented herein as this is what was required by the sponsor. The method used to identify the flow rate which induces plastic plate deformation was a staggered increasing stair step of flow rate over the duration of the test until deformation was observed via strain gage readout. A graphical sketch of flow rate and plate strain versus time, shown in figure 3, outlines an example of this overall process. An initial flow rate at the baseline equilibrium state was reached (SP-0). Upon reaching the test's initial conditions for a minimum of approximately 30 minutes the following procedure was performed

1. Increase flow rate. Flow rate was increased by five gpm over previous increase (initially SP-1), while simultaneously collecting a 10-second data burst, and observing the plate's strain (this incremental step size of five gpm is driven by the total flow error of the pump head and its hysteresis).
2. Maintain upper flow rate. After a minimum of five minutes at SP-1 equilibrium, a second 10-second burst acquisition was completed.
3. Reduce flow rate. The flow rate was decreased back to SP-0, while simultaneously collecting a third 10-second data burst, and the plate's strain was observed.
4. Assess condition of the plate. If the plate's yield stress was not reached the plate's deformation should remain in the elastic state and therefore return to its original strain readout at initial SP-0 state. SP-0 was maintained for a minimum of five minutes and a 10-second data burst shall be collected before proceeding either back to Step 1 and increasing the upper flow rate set-point or concluding the test.

The process described in steps 1-4 was continue until the observation of the plate's strain is noticeably increased over the initial SP-0 strain, as shown in figure 3; notice in the figure that although the flow rate decreased to the baseline equilibrium state, the strain does not. This provides evidence that plastic deformation took place and was induced by hydraulic loads imposed between flow rates of SP-2 and SP-3 (or SP-(n-1), and SP-n, as the case may be). Upon observation of plastic deformation through strain gage readout, the HMFTF was brought to a shutdown and standby state, the test section was disassembled from the primary loop piping system and an inspection of the center channel in the GTPA was conducted using

a channel gap probe (CGP). Upon verification that the plate(s) did go through plastic deformation as determined by the CGP, the test was determined complete.

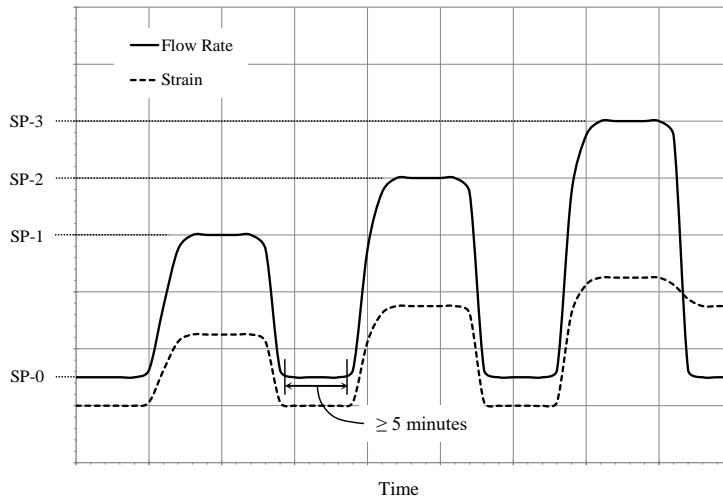


FIG 3 – Sketch of bulk flow rate and plate strain versus time

Figure 4 provides a summary of the critical thermal hydraulic instruments during the conduct of the test. Note that all control variables during the test remained within their required nominal range. No anomalous observations were made resulting from the hydraulic boundary conditions imposed on the GTPA during the duration of the test.

The outcome of averaging each step and comparing it against its corresponding pressure drop is shown in figure 7(a). The data presented in figure 7(a) include all measurement uncertainty and 2 standard deviations of stochastic uncertainty, leading to a 95 percent confidence in the values presented with error bars. A quadratic trend line has been fit to figure 7(b). The proportionality between pressure drop and the square of flow assumes all other parameters to be constant. While density of the fluid is maintained nearly constant throughout the duration of the test by controlling the pressure and temperature fluid state properties; friction factor is dependent upon the fluid velocity and attributes of the geometry, and may therefore not hold constant over the entire range tested. Regardless, a linear relation is also shown in figure 7(b) between the square of flow rate and that of pressure drop through the element. Note that both trend lines hold an  $R^2$  value of greater than 0.9998.

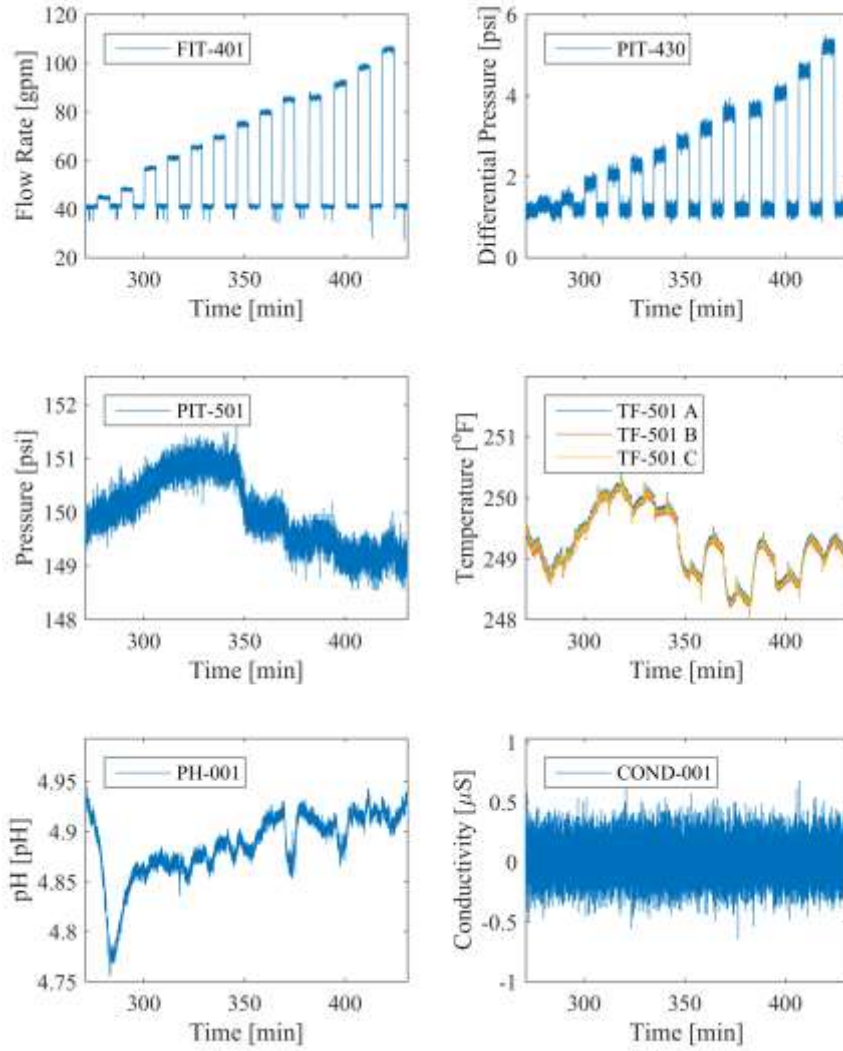


FIG 4 – Flow Test Figures of Merit

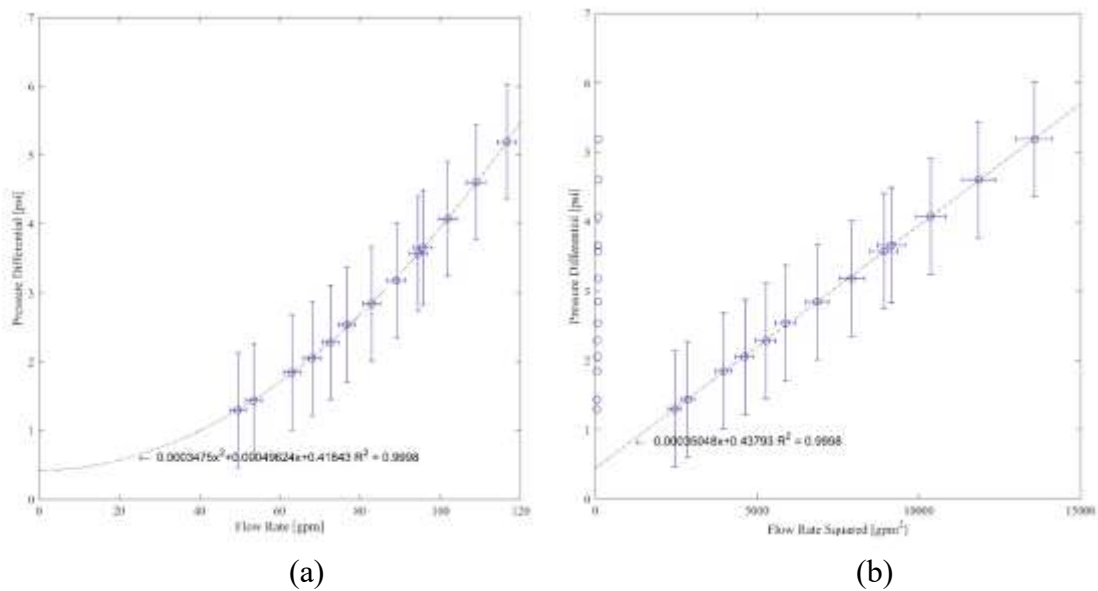


FIG 5 – (a) Flow and pressure drop comparison and (b) flow and pressure drop quadratic relationship

Note that two pressure tubes are located in each flow channel when the experiment is configured in its testing orientation. One of these pressure tubes is aligned to measure total pressure, the other is aligned to meter static pressure. The estimated inferred velocity within each channel may be computed from the pressure difference of pitot tubes located in each channel through Bernoulli's relation

$$\frac{v_1^2}{2} + \frac{P_1}{\rho} + h_1 g_1 = \frac{v_2^2}{2} + \frac{P_2}{\rho} + h_2 g_2. \quad (1)$$

Here, it is assumed that the difference in the body force is negligible, and the stagnation velocity ( $v_2$ ) is null. Then, equation 3 may be reformulated as the estimated velocity in a respective channel ( $v_i$ ) as

$$v_i = \left( \frac{2(P_t - P_s)_i}{\rho} \right)^{\frac{1}{2}} \quad (2)$$

where  $P_t$  is the total pressure (formerly  $P_2$ ) and  $P_s$  is the static pressure (formerly  $P_1$ ). Considering the computing of velocity shown in equation (2) the velocity for each channel at a total respective flow rate may be tabulated. In order to achieve the highest fidelity in the measured velocity, the pitot tube pressure values were corrected for a baseline 0 velocity at temperature and pressure. This was achieved by ensuring the calculated velocity was 0 at operating conditions and no flow (occurring at 210-212 minutes). This correction was performed immediately following shut off of the pump after the stair step was completed.

Figure 6 presents the local estimated superficial velocity in channels 1 through 7 of each respective channel within the GTPA for each flow rate steps that was tested. Note that the plates are symmetric about channel 4; therefore it may be assumed that the local velocity acquired in channel 3 and 5 should approximate one another, similarly 1 and 7, and 2 and 6 should be similar. Since all channels are nominally the same size, they should be approximately the same velocity with higher channel velocities near the center. As can be seen in figure 7 this generally holds true. The exception being channel 1 whose pitot tubes failed due to fretting.

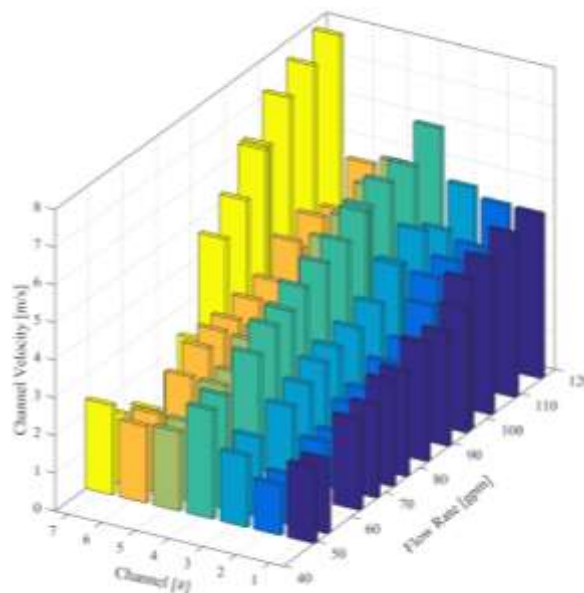


FIG 6 – Coolant channel inferred velocity

An estimate of volumetric flow rate within a given channel ( $Q_i$ ) may be synthesized from the flow cross-sectional area ( $A$ ) and the fluid superficial velocity

$$Q_i = \bar{v}_i \cdot A_i \quad (3)$$

It should be noted, the superficial velocity and the pitot tube measured velocity are not the same. The measured velocity is dependent upon the location of the total pressure pitot tube, thus the superficial velocity is dependent upon the measuring location and flow conditions. The superficial velocity is determined as,

$$\bar{v}_i = C_i \cdot v_i \quad (4)$$

where  $C_i$  is a correction factor. For fully developed laminar flow between parallel plates, the value is furthest from unity. The velocity profile for a rectangular channel is

$$u(y, z) = \frac{16a^2}{\mu\pi^3} \left( -\frac{d\hat{p}}{dx} \right) \sum_{n=1,3,5,\dots}^{\infty} (-1)^{(n-1)/2} \left[ 1 - \frac{\cosh(n\pi z / 2a)}{\cosh(n\pi b / 2a)} \right] \frac{\cos(n\pi y)}{n^3} \quad (5)$$

where  $(-a \leq y \leq a)$  and  $(-b \leq z \leq b)$ . Integration of equation (5) provides a value for the flow rate which can be converted to an average velocity and solution of (5) at the origin provides the maximum velocity. While a function of fluid properties and geometry, the correction factor for laminar flow is approximately 2/3.

As flow becomes turbulent and the Reynolds number increases, the correction factor asymptotically approaches unity (the value derived via inviscid flow theory). Since the correction factor is not explicitly known, the value for the centerline velocity can be approximated using the log-law for parallel plates,

$$\frac{u_{max}}{v^*} \cong \frac{1}{\kappa} \ln \left( \frac{h v^*}{2\nu} \right) + B, \text{ where } \kappa \approx 0.41 B \approx 5.0 \quad (6)$$

The log law provides a value for the average value defined as,

$$\bar{u}_{ave} \cong v^* \left( \frac{1}{\kappa} \ln \left( \frac{h v^*}{2\nu} + B - \frac{1}{\kappa} \right) \right) \quad (7)$$

The two previous equations can be iterated upon to determine the value of  $C_i$  for any given channel at any given state, nominally it has a value of 0.78.

Additionally, each flow channel's total nominal flow cross section may be computed by

$$A_i = s w_i - \frac{\pi}{4} d_1^2 - \frac{\pi}{4} d_2^2 \quad (8)$$

where  $s$  is the span of the channel,  $w_i$  is the channel width,  $d_1$  is the diameter of the total-pressure pitot tube and  $d_2$  is the diameter of the static-pressure pitot tube. Both pitot tubes were fabricated from the same tube-extrusion, and therefore assumed to have the same nominal characteristics; thus

$$A_i \cong s w_i - \frac{\pi}{2} d_1^2. \quad (9)$$

The volumetric flow rate within a given channel may then be computed by

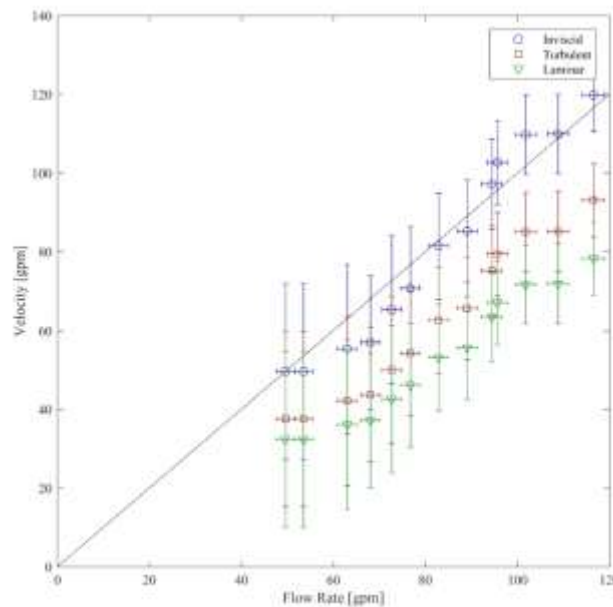
$$Q_i = \left( s w_i - \frac{\pi}{2} d_1^2 \right) \left( \frac{2(P_t - P_s)_i}{\rho} \right)^{\frac{1}{2}}. \quad (10)$$

Then the sum of flow rates computed from each channel yields the estimated total flow rate passing through all channels, or the total estimated flow rate passing through the capsule ( $Q_{total}$ ),

$$Q_{total} = \sum_{i=1}^n Q_i, \quad (11)$$

Note that the FSP-1 outer and inner baskets are placed within the Flow Simulator and held in position via gravity and fluid body forces. The experimental geometry has been designed to allow for the majority of flow to pass through the inner basket. A small portion of flow may still bypass the primary path and flow around the outside of either the inner or outer basket. Flow through the inner basket is restricted by the instrumented channel i.e. the channel with the pitot tubes. Although it is known that flow will be greater in the non-instrumented channel, the quantity of the diverted flow is not known. One may infer this quantity by comparing the total net flow rate measured through the test section from FIT-401 and comparing it against the total estimated flow calculated to pass through each capsule via equation (11).

A direct comparison between these inferred flow rate and measured flow rate values are shown in figure 7 explicitly. The solid line in figure



7

FIG 7 – represents a unity relationship between the total measured flow and the inferred flow rate. Recall that the pitot tube in channel 1 failed to respond proportionally which results in a flow rate which approximates the measured flow rate but doesn't explicitly duplicate it. This is evident in the sudden drop in the inferred flow rate values presented in the below figure after the second data point.

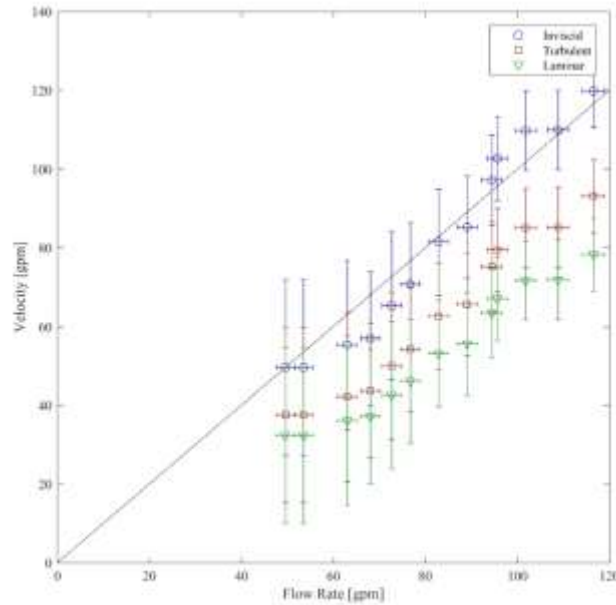


FIG 7 – Computed flow comparison to test flow rate

Figure 7 shows a comparison for the uncorrected velocity calculated by the pitot tubes. If a correction is to be considered, there are a few options. Inviscid theory provides the average velocity as being equivalent to the measured velocity. Laminar flow diverges from the measured velocity most significantly. The laminar values are calculated from the solution for fully-developed laminar flow in a rectangular duct of the provided shape and size of the channels (see equation (5)). In the case of turbulent flow, the log-law approximation for infinite channels is used (see equation (7)). In theory, the log-law channel approach is closest at predicting the ratio between average and centerline velocity. The maximum velocity is approximately 1.29 times greater for the parallel plate case in turbulent flow (compared to 1.6 for the laminar case). The results are also detailed in figure 7.

Note that data falling on the 1:1 line would represent all flow through the center channels of the experiment, however this should not be representative of the actual flow distribution within the experiment. Several possible paths exist within the experiment for bypass flow that would not be measured by the pitot tubes.

Strain gages were bonded to the test plate at six unique locations. Three partner-sets were bonded near the leading edge (SR-417AC, SR-417BD), along the axial middle region (SR-418AC, SR-418BD), and near the trailing edge of the plate (SR-419AC, SR-419BD). Strain gages SR-417AC and SR-417BD produced dissimilar output signals during the conduct of the test within the time domain as shown in figure 8. SR-417AC produced a relatively small change in amplitude when flow was increased and decreased respectively, while SR-417BD's response appeared not to correlate to the hydraulic loading imposed on the plate. It was therefore speculated that the temporal response of SR-417BD was unreliable in its post-test interpretation of the plate's response. All other strain gages responded acceptably during the entirety of the test. While subtle, it was found that at a total flow rate of approximately 104 gpm (417 minutes) residual strain was observed on several strain gages.

#### **4 Concluding Remarks**

This study summarizes the outcomes of a single hydraulic experiment performed within the HMFTF at OSU that supports efforts to qualify a new fuel prototype under the Fuels Qualification Program. The paper details the process used to perform hydro-mechanical testing of prototypic plates and the methods used to quantify select outcomes. Observations were made associated with the static and dynamic response of the test plate exposed to both steady and transient boundary conditions. A more comprehensive understanding was acquired of the dynamic instability of a plate under transient loading as its relation to lock-in flow rate. Additionally, insights were provided toward the outcomes of these test and the aggregate of other tests within the campaign that have been performed up to this point. The outcome of all tests performed in support of the Fuel Qualification Program will go to provide an objective basis on the overall stability and limits of the stability of the new prototypic fuel and the relative comparison of this fuel to presently used fuel within plate-type research reactors.

#### **5 Acknowledgements**

Prepared for the U.S. Department of Energy Office of NNSA/NA-23 Material Management and Minimization under DOE Idaho Operations Office Contract DE-AC07-05ID14517  
Disclaimer – This information was prepared as an account of work sponsored by an agency of the U.S. Government. Neither the U.S. Government nor any agency thereof, nor any of their employees, makes any warranty, express or implied, or assumes any legal liability or responsibility for the accuracy, completeness, or usefulness of any information, apparatus, product, or process disclosed, or represents that its use would not infringe privately owned rights. References herein to any specific commercial product, process, or service by trade name, trademark, manufacturer, or otherwise, does not necessarily constitute or imply its endorsement, recommendation, or favoring by the U.S. Government or any agency thereof. The views and opinions of authors expressed herein do not necessarily state or reflect those of the U.S. Government or any agency thereof.

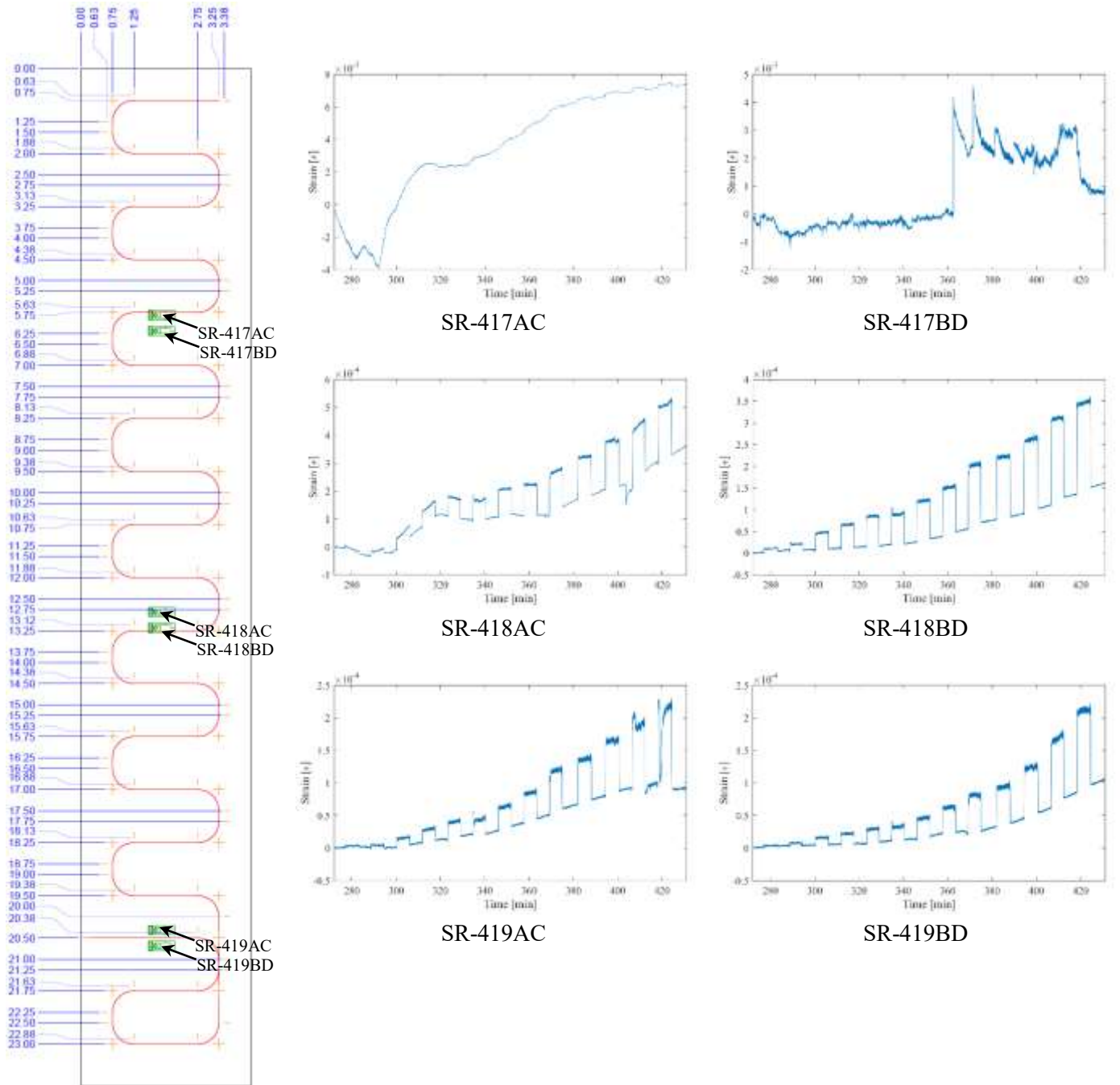


FIG 8 – Temporal response of strain gages

## 6 References

- [1] Marcum, W.R., *OSU HMFTF Facility Description Report*, Oregon State University, 2016.
- [2] Savino, J.M. and C.D. Lanzo, *Techniques Used to Measure the Hydraulic Characteristics of the NASA Plum Brook Reactor*, D-1725, Editor. 1963, National Aeronautics and Space Administration: Cleveland.